NeuroImage 231 (2021) 117850

Contents lists available at ScienceDirect

NeuroImage

journal homepage: www.elsevier.com/locate/neuroimage

Higher-order sensorimotor circuit of the brain's global network supports human consciousness

Pengmin Qin[a,b,1,*], Xuehai Wu[b,c,d,e,1], Changwei Wu[f,g,h], Hang Wu[a], Jun Zhang[i], Zirui Huang[j], Xuchu Weng[k], Di Zang[c,d,e], Zengxin Qi[c], Weijun Tang[l], Tanikawa Hiromi[c], Jiaxing Tan[c], Sean Tanabe[j], Stuart Fogel[m], Anthony G. Hudetz[j], Yihong Yang[n], Emmanuel A Stamatakis[o], Ying Mao[c,**], Georg Northoff[p,q]

[a] *Key Laboratory of Brain, Cognition and Education Sciences, Ministry of Education; School of Psychology, Center for Studies of Psychological Application, and Guangdong Key Laboratory of Mental Health and Cognitive Science, South China Normal University, Guangzhou, Guangdong, 510631, China*
[b] *Pazhou Lab, Guangzhou 510335, China*
[c] *Department of Neurosurgery, Huashan Hospital, Shanghai Medical College, Fudan University, Shanghai, China*
[d] *Shanghai Clinical Medical Center of Neurosurgery, Shanghai Key laboratory of Brain Function Restoration and Neural Regeneration, Neurosurgical Institute of Fudan University, Shanghai, China*
[e] *State Key Laboratory of Medical Neurobiology and MOE Frontiers Center for Brain Science, School of Basic Medical Sciences and Institutes of Brain Science, Fudan University, Shanghai, China*
[f] *Research Center for Brain and Consciousness, Taipei Medical University, Taipei, Taiwan*
[g] *Graduate Institute of Humanities in Medicine, Taipei Medical University, Taipei, Taiwan*
[h] *Shuang-Ho Hospital, Taipei Medical University, New Taipei, Taiwan*
[i] *Department of Anesthesiology, Fudan University Shanghai Cancer center, Shanghai, China*
[j] *Department of Anesthesiology and Center for Consciousness Science, University of Michigan, Ann Arbor, MI, USA*
[k] *Institute for Brain Research and Rehabilitation, South China Normal University, Guangzhou, Guangdong, China*
[l] *Radiology Department, Shanghai Huashan Hospital, Fudan University, Shanghai, China*
[m] *School of Psychology, University of Ottawa, Ottawa, Canada*
[n] *Neuroimaging Research Branch, National Institute on Drug Abuse, Intramural Research Programs, National Institutes of Health, Baltimore, USA*
[o] *Division of Anaesthesia, School of Clinical Medicine, University of Cambridge, Cambridge, UK*
[p] *Institute of Mental Health Research, University of Ottawa, Ottawa, Ontario, Canada*
[q] *Mental Health Centre, Zhejiang University School of Medicine, Hangzhou, China*

ARTICLE INFO

Keywords:
Anesthesia
Degree centrality
Inferior parietal lobule
Rapid eye movement sleep
Higher-order sensorimotor circuit
Disorders of consciousness

ABSTRACT

Consciousness is a mental characteristic of the human mind, whose exact neural features remain unclear. We aimed to identify the critical nodes within the brain's global functional network that support consciousness. To that end, we collected a large fMRI resting state dataset with subjects in at least one of the following three consciousness states: preserved (including the healthy awake state, and patients with a brain injury history (BI) that is fully conscious), reduced (including the N1-sleep state, and minimally conscious state), and lost (including the N3-sleep state, anesthesia, and unresponsive wakefulness state). We also included a unique dataset of subjects in rapid eye movement sleep state (REM-sleep) to test for the presence of consciousness with minimum movements and sensory input. To identify critical nodes, i.e., hubs, within the brain's global functional network, we used a graph-theoretical measure of degree centrality conjoined with ROI-based functional connectivity. Using these methods, we identified various higher-order sensory and motor regions including the supplementary motor area, bilateral supramarginal gyrus (part of inferior parietal lobule), supragenual/dorsal anterior cingulate cortex, and left middle temporal gyrus, that could be important hubs whose degree centrality was significantly reduced when consciousness was reduced or absent. Additionally, we identified a sensorimotor circuit, in which the functional

* Corresponding author at: Key Laboratory of Brain, Cognition and Education Sciences, Ministry of Education; School of Psychology, Center for Studies of Psychological Application, and Guangdong Key Laboratory of Mental Health and Cognitive Science, South China Normal University, Guangzhou, Guangdong, 510631, China.
** Corresponding author at: Department of Neurosurgery, Huashan Hospital, Shanghai Medical College, Fudan University, Shanghai, China.
E-mail addresses: qin.pengmin@m.scnu.edu.cn (P. Qin), maoying@fudan.edu.cn (Y. Mao).
[1] These authors contributed equally to this work.

https://doi.org/10.1016/j.neuroimage.2021.117850
Received 16 October 2020; Received in revised form 29 December 2020; Accepted 8 February 2021
Available online 12 February 2021

connectivity among these regions was significantly correlated with levels of consciousness across the different groups, and remained present in the REM-sleep group. Taken together, we demonstrated that regions forming a higher-order sensorimotor integration circuit are involved in supporting consciousness within the brain's global functional network. That offers novel and more mechanism-guided treatment targets for disorders of consciousness.

1. Introduction

Consciousness is a complex mental characteristic which has been the focus of intensive investigation in neuroscience (Bachmann, 2015; Koch et al., 2016; Tononi et al., 2016), and its underlying neural features are not yet fully clarified (Crick and Koch, 2003). Studies employing various methodologies including functional magnetic resonance imaging and multichannel electroencephalography so far have yielded conflicting views on whether resting state and task-evoked activity of specific sensory and cognitive brain regions my serve as the neural correlates of consciousness (NCC), such as the posterior "hot zone" (Koch et al., 2016) or the dorsolateral prefrontal (Dehaene and Changeux, 2011). In addition to specific regions and regional specialization, the long-distance communication among remote brain regions as well as global activity changes have been emphasized (Huang et al., 2016; Luppi et al., 2019; Tanabe et al., 2020; Tang et al., 2017). Efforts have been directed to identifying the particular regions of the brain's global functional network, which in graph theoretical terms are called "hubs", may be critical in supporting consciousness. Hubs or nodes reflect local activity in specific regions that strongly modulate the brain's global activity (Boly et al., 2017). While recent approaches identified the dynamic nature of the NCC (Demertzi et al., 2019), the regions and circuits that support consciousness within the brain's global functional network remain yet unclear.

Clinically, consciousness has been determined by dimensions like level/state and content (Laureys, 2005; Northoff, 2014). While the neural features of the level/state of consciousness have been mainly investigated in disorders of consciousness, the neural features of the content of consciousness are mainly probed in healthy fully awake subjects employing conscious vs unconscious stimulus/task presentations (Northoff and Lamme, 2020). Insights into the consciousness as a state have strongly benefited from investigations of abnormal behavioral and brain states characterized by reduced or absent consciousness, e.g., in anesthesia (Hashmi et al., 2017; Kertai et al., 2012; Monti et al., 2013; Moon et al., 2015), sleep (Horovitz et al., 2009; Houldin et al., 2019; Hu et al., 2020; Larson-Prior et al., 2009), unresponsive wakefulness syndrome (UWS) and minimally conscious state (MCS) (Engemann et al., 2018; Monti et al., 2010; Schiff, 2015). One particularly powerful approach is to combine the various unconsciousness states (N3-sleep, anesthesia and UWS) to identify brain regions and networks whose activity patterns could track the variations in the behaviorally defined states of consciousness. Several previous studies had combined all or two of the three unconsciousness-states (sleep, anesthesia and UWS) to investigate the stimulus-induced brain activity change (Casali et al., 2013) or brain resting-state connectivity change from consciousness to unconsciousness (Huang et al., 2018, 2020; Luppi et al., 2019). Therefore, the predominant focus of the current study is on the level/state of consciousness, as when comparing anesthesia, N3-sleep, and UWS may thus provide the brain's resting state with the capacity to exhibit a certain level/state of consciousness.

Prior investigations, in UWS, sleep or anesthesia, have demonstrated abnormal activity or connectivity in higher-order sensory and motor regions like supplementary motor area (SMA) and inferior parietal lobule (IPL) (Amico et al., 2017; Demertzi et al., 2015; Liu et al., 2017; Martínez et al., 2020; Mitra et al., 2015; Owen et al., 2006; Qin et al., 2010; Zhang et al., 2018b), while the stimulus evoked activity of primary sensory regions is largely preserved (Di et al., 2007). These studies suggested that sensorimotor integration may be required for normal, healthy consciousness (Amico et al., 2017; O'Regan and Noe, 2001). The findings highlighted a key role for a higher-order sensorimotor integration circuit in supporting consciousness. However, additional higher-order regions and functional networks like the salience network (Qin et al., 2015), default-mode network (Vanhaudenhuyse et al., 2010), and frontal-executive network (Stender et al., 2014) have also been implicated in states of reduced or absent consciousness. Some studies even suggest that the brain's global spatial activity pattern that operates across the whole brain may be central in supporting consciousness (Tanabe et al., 2020). These findings on local and global activity changes led to the focus of the current study: to find out how these changes can be reconciled in support of consciousness. Specifically, we asked whether consciousness is supported by the existence of a higher-order sensorimotor integration circuit within the brain's global functional network.

To address the above question, degree centrality (DC), a graph theoretical measure, is a useful tool. Based on the resting-state fMRI data, degree centrality allows measuring the relative importance and contributions of specific regions serving as nodes within the global overall network architecture by calculating the number of connections made to a node (voxel) (van den Heuvel and Sporns, 2013). This approach is suitable for calculating the degree of functional integration (centrality) of hubs in a complex network such as the brain. Brain regions with high degree centrality and their functional connections are thought to allow for higher-order integration of different inputs like sensory and motor, i.e., higher-order sensorimotor integration (Bullmore and Sporns, 2012).

In this study, we aim to identify the higher-order integration nodes forming a circuit within the brain's global functional network using resting-state fMRI. Importantly, we aim to show how such circuit can track behaviorally defined states of consciousness from normal wakefulness to pharmacological and neuropathological states where consciousness was presumed to be reduced or lost. We take advantage of a large dataset that included subjects in anesthesia, sleep, and patients with disorders of consciousness (DOC, including UWS and MCS). Most importantly, we also included a unique fMRI dataset on REM-sleep, where sensory input is maximally reduced and the ability of intentional movement generation/execution is lost while the subjects still maintain rich conscious experiences, i.e. dream. Although the contents of the dream state occur in rather bizarre and often distorted contexts like the famous clock by Dali (which he painted after being woken up from a dream), dream states show a level/state of consciousness that is more or less comparable to the one of the awake state (Chow et al., 2013). Investigating REM-sleep will thus provide a unique window into understanding the NCC by itself, independent of sensory and motor processing. This is particularly important because REM-sleep will be helpful to exclude the possibility of effects caused by a lack of mobility, since unconscious states are also characterized by immobility (e.g. sleep, anesthesia, and UWS). REM-sleep on the other hand, also helps excluding the possibility of effects caused by a lack of environmental sensory inputs, since REM-sleep and unconscious states share the same disconnection from the external world.

Specifically, the current study includes the following datasets: a sleep group without REM (including awake state, N1-sleep, and N3-sleep, in which the N3-sleep was regarded as an unconscious state (deep sleep stage) (Laureys, 2005)), an anesthesia group (including conscious wake and anesthesia states), and DOC patients (including UWS, MCS and a fully conscious patient group with brain injury history (BI). Only patients with structurally preserved brain injuries were included) (See Supplementary Table 1, and Supplementary fig. 1 for structural brain im-

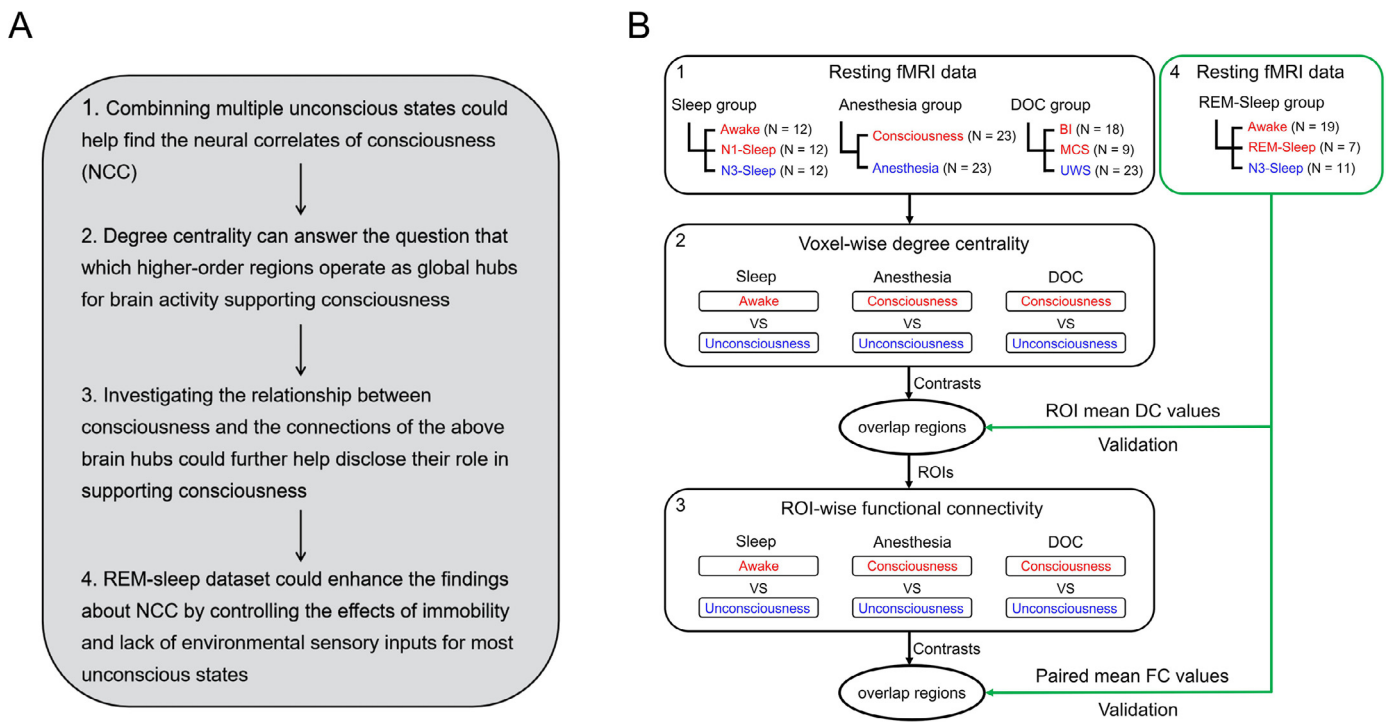

Fig. 1. The schemata for experiment design and data processing. (A) The strategy of the experiment design and data analysis. (B) The schemata for experiment design. A within-subject design was adopted for the sleep and anesthesia groups, and a between-subject design was adopted for the DOC and REM-Sleep groups. Red represents consciousness or reduced consciousness states; blue represents unconsciousness. The black square represents the exploratory datasets which were used to define the ROIs with degree centrality and functional connectivity changes during unconsciousness. The green square represents the validation datasets (REM-sleep group). DC values = degree centrality values, FC values = functional connectivity values. N: the sample size of each group. The digital number indicated the corresponding idea and data processing in panels A and B.

ages). An REM-sleep group (including awake, N3-sleep state and REM-sleep state) was also collected for verification of the effects found in the other three groups. For the data-analysis, we first tried to identify the brain regions with significant degree centrality reduction during unconsciousness, and confirmed the results with the REM-sleep dataset. The functional connections between each of these brain regions were then investigated in all levels ranging from consciousness to unconsciousness; that served the purpose to extract the functionally relevant circuit among different regions within the global functional network. See Fig. 1 for the main idea of the manuscript and the Schemata of data processing.

2. Materials and methods

2.1. Participants and data acquisition – sleep group

This dataset is from a previously published study (Tsai et al., 2014). There were 12 healthy men with regular sleep duration of 7–8 h per night and consistent bed/wake time for at least 4 days. Participants' age ranged from 20 to 27 years (mean ± SD = 23 ± 2.5 years). We conducted simultaneous EEG–fMRI recordings for the sleep protocol. EEG was recorded using a 32-channel MR-compatible system (Brain Products, Gilching, Germany). The 32 electrodes, including 30 EEG channels, one electrooculography (EOG) channel, and one electrocardiogram (ECG) channel, were positioned according to the international 10/20 system. The electrode-skin impedance was reduced to <5 kΩ using abrasive electrode paste (ABRALYT HiCl). The EEG signal was synchronized with the MR trigger and recorded using the Brain Vision Recorder software (Brain Products) with a 5 kHz sampling rate and a 0.1 μV voltage resolution. Low-pass and high-pass filters were set at 250 Hz and 0.0159 Hz, respectively, with an additional 60-Hz notch filter.

The sleep protocol was conducted at midnight and the participants were instructed to try to fall asleep after the EPI scan started. A licensed sleep technician in Kaohsiung Medical University Hospital visually scored the sleep stages for every 30 s epoch, according to the current criteria of the American Academy of Sleep Medicine (AASM). A within-subject design was adopted. Each subject had three different states: the awake state (before sleep), N1-sleep, and N3-sleep. The MR images were acquired on a 3 Tesla Siemens Tim-Trio scanner. Functional images were acquired using a T2*-weighted EPI sequence (TR/TE/θ = 2500 ms/30 ms/80°, FOV = 220 × 220 mm, matrix= 64 × 64, 35 slices with 3.4 mm thickness). A high-resolution T1-weighted anatomical image was acquired for all participants for functional image registration and localization. See the previous study for more detailed information about the EEG and fMRI data acquisition parameters and data preprocessing (Tsai et al., 2014).

2.2. Participants and data acquisition – REM-Sleep group

These datasets were from a previously published study (Fang et al., 2019) using simultaneous EEG–fMRI recordings. There were 24 healthy participants (age from 18 years to 34 years, mean ± SD = 23.8 ± 4.1 years, 9 female) included in the current analysis. Different from the sleep group, the REM-sleep group had a between-subject design. The awake-state was recorded in 19 participants (which occurred during sleep, not before sleep), the N3-state was recorded in 11 participants and the REM-sleep was recorded in seven participants. One participant had all of the awake, N3-sleep and REM-sleep states; two participants had both the N3-sleep and REM-sleep; two participants had both the awake and REM-sleep; seven participants had both the awake and N3-sleep. Each sleep state had a minimum of 90 volumes. The sleep stages were scored in the same way as sleep group 1. The MR images were acquired on a 3 Tesla Siemens Magnetom Prisma scanner. Functional images were acquired

using a T2*-weighted EPI sequence (TR/TE/θ = 2160 ms/30 ms/90°, FOV = 220 × 220 mm, matrix= 64 × 64 × 40, 40 slices with 3 mm thickness). A high-resolution T1-weighted anatomical image was acquired for all participants for functional image registration and localization. See the previous study for more detailed information about the EEG and fMRI data acquisition parameters and data preprocessing (Fang et al., 2019).

2.3. Participants and data acquisition – anesthesia group

Seventeen participants received intravenous propofol anesthesia and six subjects received inhalational sevoflurane anesthesia. The participants' age ranged from 26 years to 63 years (mean ± SD = 45.8 ± 11.8 years, 11 female). All the subjects had received the elective transsphenoidal approach for resection of pituitary microadenoma. Informed written consent was obtained from each subject. The study was approved by the Ethics Committee of Shanghai Huashan Hospital, Fudan University, Shanghai, China.

For the propofol group, we achieved a 3.0–5.0 μg/ml plasma concentration by using a target-controlled infusion (TCI) based on the Marsh model. This was followed by remifentanil (1.0 μg/kg) and succinylcholine (1 mg/kg) to facilitate endotracheal intubation. We then maintained the TCI propofol at a stable effect-site concentration (4.0 μg/ml) which reliably induced an unconscious state in the subjects. For the sevoflurane group, we gave the subjects 8% sevoflurane in 100% oxygen, adjusting fresh gas flow to 6 L/min, combined with remifentanil (1.0 μg/kg) and succinylcholine (1.0 mg/kg). This was maintained with 2.6% (1.3 MAC) ETsevo in 100% oxygen, and a fresh gas flow at 2.0 L/min. The concentration of sevoflurane successfully maintained a loss of consciousness in subjects, classified as ASA physical status I or II (Katoh and Ikeda, 1998). The anesthetic effects on the brain are considered to be solely pertaining to propofol and sevoflurane because of the quick elimination of the analgesic remifentanil and depolarized neuromuscular relaxant succinylcholine from plasma. To confirm the effects of each drug, the results for each drug were also presented separately in the supplementary materials.

During the anesthetic state, subjects were given intermittent positive pressure ventilation, with tidal volume at 8–10 ml/kg, respiratory rate at 10–12 beats per minute, and $PetCO_2$ (end tidal partial pressure of CO_2) at 35–37 mmHg. All subjects met the criteria of deep sedation: neither a response to verbal commands ("squeeze my hand"), nor a response to prodding or shaking was observed during anesthesia, corresponding to Ramsay 5–6 and an OAA/S score of 1. In addition, no subject reported explicit memory in the post-operative follow-up. Therefore, all subjects were considered unconscious during anesthesia. A within-subject design was adopted. Each subject had two states: consciousness and anesthesia. See the previous study for the detailed information of the anesthesia protocols (Huang et al., 2016; Zhang et al., 2018a).

All the datasets had the same fMRI acquisition parameters. A Siemens 3T scanner used T2*-weighted EPI sequence to acquire functional images of the whole brain (TR/TE/θ= 2000 ms/30 ms/90°, FOV = 192 mm, matrix size = 64 × 64, 25 slices with 6-mm thickness, gap = 0 mm, 240 scans). A high-resolution T1-weighted anatomical image was also acquired for all participants. EPI data acquisition was conducted both in wakefulness prior to anesthesia and in the anaesthetized state. The subjects were instructed to relax and keep their eyes closed during scanning. Following this, subjects were anaesthetized and given full hydration with hydroxyethyl starch to avoid hypotension. The anaesthetized state resting-state fMRI scan was performed fifteen minutes after stabilization of anaesthetic levels and hemodynamics.

2.4. Participants and data acquisition –patients with disorders of consciousness

To minimize the effects of structural distortion and maintain local neural integrity for the degree centrality analysis, we included 50 structurally well-preserved brain injury patients with three different conditions: UWS, MCS and BI. These structurally well-preserved patients, who were selected by author XW and then checked by author PQ according to their structural images, had limited brain lesions and limited brain structure distortion (Supplementary Table 1 for detailed demographic and clinical information, and Supplementary fig. 1 for representative patient's structural image). The UWS and MCS patients were assessed using the Coma Recovery Scale-Revised (CRS-R) (Giacino et al., 2004) before the fMRI scanning. Informed written consent was obtained from the patients' legal representatives. The study was approved by the Ethics Committee of Shanghai Huashan Hospital, Fudan University, Shanghai, China.

For the datasets in the current study, the MR images were acquired on the same Siemens 3 Tesla scanner. Functional images were acquired using a T2*-weighted EPI sequence (TR/TE/θ = 2000 ms/35 ms/90°, FOV = 256 × 256 mm, matrix= 64 × 64, 33 slices with 4-mm thickness, gap = 0 mm, 200 scans). Each volume had 33 axial slices, covering the whole brain. Two hundred volumes were acquired during rest. A high-resolution T1-weighted anatomical image was acquired for all participants for functional image registration and localization. All participants were given the same instructions, in which they were told to take a comfortable supine position, relax, close their eyes, and not concentrate on anything in particular during the scanning. Nevertheless, please note that due to their cognitive and physical impairments, a persistent awake state with eyes closed cannot be guaranteed for the MCS and UWS patients throughout the scanning (Rudas 2019). All participants wore earplugs to minimize the noise of the scanner.

2.5. Data preprocessing

Anatomical images from the two sleep groups, anesthesia, and patient with DOC were segmented into grey matter (GM), white matter (WM), and cerebrospinal fluid (CSF), using the FAST tool from the FSL software package (http://www.fmrib.ox.ac.uk/fsl/). Functional images were processed using the AFNI software package. After discarding the first two volumes, functional images underwent a preprocessing procedure which included: slice-timing correction; head-motion correction; masking for the removal of the skull; and spatial smoothing using a 6-mm kernel. Time-series were then intensity normalized by computing the ratio of the signal in each voxel at each time point to the mean across all time points, and then multiplied by 100. The six estimated head motion parameters and the mean time-series from the white matter (WM) and the cerebrospinal fluid (CSF), which were defined using partial volume thresholds of 0.99 for each tissue type, were considered as noise covariates and were regressed out from the data. The data were bandpass filtered preserving signals between 0.01 and 0.08 Hz. Functional images from all the three groups were transformed into MNI standard space (3 × 3 × 3 mm^3 resolution).

For all the datasets, the issue of head motion was rigorously addressed, as minor differences in motion have been shown to cause artificial group differences (Power et al., 2012). Motion was quantified as the Euclidean distance calculated from the six rigid-body motion parameters for two consecutive time points (AFNI, 1d_tool.py). Any instance of movement greater than 0.5 mm was considered excessive, for which the respective volume as well as the immediately preceding and subsequent volumes were removed. In order to obtain reliable results, only participants with more than 90 volumes (Yan et al., 2013) remaining were included for the sleep group (Awake: mean ± SD = 142 ± 1 volumes; N1-sleep: mean ± SD = 146 ± 41 volumes; N3-sleep: mean ± SD = 143 ± 26 volumes), for the anesthesia group (Consciousness: mean ± SD = 234 ± 8 volumes; Anesthesia: mean ± SD = 236 ± 7 volumes), for DOC group (BI: mean ± SD = 194 ± 16 volumes; MCS: mean ± SD = 181 ± 31 volumes; UWS: mean ± SD = 182 ± 27 volumes), and for REM-Sleep group (Awake: mean ± SD = 237 ± 88 volumes; N3-sleep: mean ± SD = 302 ± 199 volumes; REM-sleep: mean ± SD = 419 ± 334 volumes).

2.6. Degree centrality changes in different conscious levels

Based on the graph theory and network analysis, the degree centrality of a node reveals how many edges it has with other nodes. In the current analysis, each voxel was treated as a node, and each functional connection (Pearson correlation) between the voxel (i.e. node) and any other voxel was defined as an edge. Using the 3dTcorrMap program in AFNI, voxel-wise degree centrality was computed within a mask including grey matter (Yeo et al., 2011) and thalamus and other subcortical regions from AAL 90 template. Specifically, the correlation between any pair of voxels was calculated and voxel-wise correlation matrices were generated for every participant. In order to obtain a binary and undirected adjacency matrix, a threshold at $r > 0.3$ was applied. Voxel-wise degree centrality was then calculated by counting the number of edges connecting each voxel. To further validate the effect of different thresholds, we also calculated degree centrality at $r > 0.2$ and $r > 0.4$ separately.

For the sleep group, awake and N1-sleep were regarded as consciousness or reduced consciousness states while N3-sleep as an unconscious state (Laureys, 2005); for the anesthesia group, awake consciousness was the conscious state while anesthetic state was an unconscious state. For the DOC group, the BI and MCS were regarded as consciousness or reduced consciousness states while UWS as an unconscious state. For REM-sleep group, the awake and REM-sleep were regarded as consciousness or reduced consciousness states while N3-sleep as unconscious state.

In order to identify the common brain regions with degree centrality changes during unconscious states, paired sample t-tests were performed to compare voxel-wise differences between unconscious and conscious states for the anesthesia group. For the sleep group, repeated measures one way ANOVA was applied to analyze the difference of degree centrality values between unconscious and conscious/reduced conscious states with the AFNI program (3dMVM); within ANOVA analysis, two contrasts for consciousness vs. unconsciousness (awake vs. N3-sleep, N1-sleep vs. N3-sleep) were performed. For the DOC group, one way ANCOVA was applied to analyze the voxel-wise contrasts of degree centrality values using the 3dMVM program in AFNI, in which age, gender, head motion, the length of time since brain injury, and the length of BOLD signal series were regarded as covariates; within ANCOVA analysis, two contrasts for consciousness vs. unconsciousness (BL vs. UWS, MCS vs. UWS) were performed. All tests above were two-tailed. For all these voxel-wise contrasts, a cluster-level significance threshold of $p < 0.05$ after FWE correction ($p < 0.005$ uncorrected, cluster size > 20 voxels, 3dClusterSim, AFNI) was used. For each contrast, a binary brain map was then generated where value 1 indicated voxels of significant reduction during unconsciousness. To determine common brain regions with reduced degree centrality during unconsciousness in the anesthesia group, sleep group and DOC group, overlapping clusters (volume > 20 voxels) were computed from the binary maps obtained from the above steps. Specifically, the 3dcalc program in AFNI was used to obtain intersected voxels from all binary contrast maps, yielding clusters defined as brain hub regions for further analysis. The coordinate of the cluster centroid was regarded as the cluster center in the following analysis.

For each common brain region with degree centrality reduction during unconsciousness in the sleep group, anesthesia group and DOC group, the coordinates of cluster centers were used to make ROIs (sphere with $r = 8$ mm). Then for the REM-sleep group, mean degree centrality values within these ROIs were computed, respectively. To account for the relatively small sample size of the REM-sleep state, and to keep the statistical analysis consistent among all the groups, non-parametric statistics was used for all the following ROI-based data analysis. For each ROI, the Kruskal-Wallis H test was applied to analyze the contrasts of degree centrality values; post-hoc test included: N3-sleep vs. REM-sleep, N3-sleep vs. Awake, and REM-sleep vs. awake. All tests above were two-tailed. The effect size was estimated using η_H^2. The FDR correction was used to control for the multiple comparison problem across all 15 post-hoc tests among the five brain regions in the REM-sleep group.

2.7. Functional connectivity changes between brain regions with decreased degree centrality during unconscious states

Following the degree centrality analysis, ROI-based functional connectivity was performed with the ROIs obtained from the above analysis which showed degree centrality reduction in unconsciousness. Mean time-series from each ROI was calculated, and then the Pearson correlation coefficient was computed for each pair of regions for each condition within each group. Fisher's Z transformation was used to transform the correlation r-values to normally distributed Z-values, which were then compared between unconscious and conscious states. To test whether the relationship among all the pairs of functional connectivity was consistent during consciousness states, the correlations between the functional connectivity z-values during consciousness or awake states from one group and the values during the consciousness states from the other groups were calculated using the Spearman's correlation. The above 6 p-values were FDR corrected.

Additionally, the relationship between the mean functional connectivity z-value among all the pairs of ROI connections and levels of consciousness states were investigated in the sleep group, DOC group and REM-sleep group using the Spearman's correlation. Similar as the above whole-brain voxel-wise degree centrality, here among the five ROIs, the functional connectivity with a z-value (> 0.3095) (r value = 0.3) was also regarded as an edge, the relationship between the total edge number among the five brain regions and levels of consciousness was also investigated using Spearman's correlation. The above 6 p-values were FDR corrected. The anesthesia group was not included in this correlation analysis since it only included two levels of consciousness.

Finally, to determine the functional connectivity changes from consciousness to unconsciousness, the Wilcoxon signed-rank test was performed for each pair of ROIs in the anesthesia group. For the sleep group, the Friedman's test was performed to compare the functional connectivity between each pair of ROIs among awake, N1-sleep, and N3-sleep. For the DOC patients, the Kruskal-Wallis H test was applied to analyze the functional connectivity between each pair of ROIs among the UWS, MCS, and BI. For the REM-sleep group, the Kruskal-Wallis H test was also applied to analyze the functional connectivity between each pair of ROIs in the N3-sleep, REM-sleep and awake group. All the tests above were two-tailed, and corrected for multiple comparisons using the FDR correction, respectively. For all the statistics, degree centrality values or functional connectivity values beyond the range (mean±2SD) of each group were excluded.

3. Results

3.1. Reduced degree centrality in unconsciousness

As a first step, whole brain voxel-wise degree centrality analysis was performed to build a degree centrality map ($r > 0.3$ was taken as one edge). All the contrasts between conscious/reduced-conscious states and unconscious states showed brain regions with significant degree centrality reduction during unconscious states ($p < 0.05$ FWE correction), which overlapped in the supplementary motor area (SMA), the left supramarginal gyrus (LSMG), the right supramarginal gyrus (RSMG), the supragenual anterior cingulate cortex (SACC) and the left middle temporal gyrus (LMTG) among the sleep, anesthesia and DOC groups (Fig. 2 and supplementary Table 2). These five regions did not show any degree centrality difference between N1-sleep and awake-states in the sleep group. LSMG showed significant differences between BI and MCS, but not other four regions (Supplementary fig. 2).

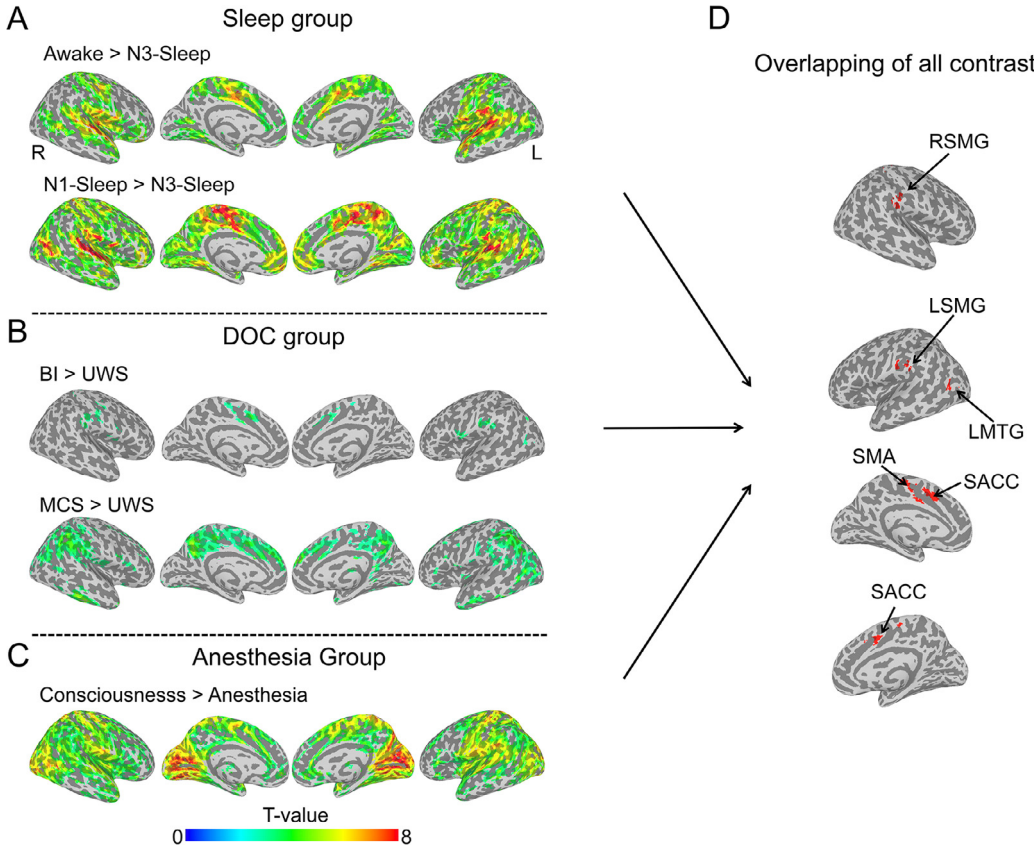

Fig. 2. The brain regions with decreased degree centrality during unconsciousness. All the degree centrality contrasts for unconscious < conscious/reduced conscious states, (A) Sleep group, (B) DOC patient group and (C) anesthesia group. The activated clusters with ($p < 0.005$ uncorrected, volume > 20 voxels) are displayed. (D) The overlapped brain regions (volume > 20 voxels) of all the contrasts from panel A, B, and C. SMA = supplementary motor area; LSMG = left supramarginal gyrus; RSMG = right supramarginal gyrus; LMTG = left middle temporal gyrus; SACC = supragenual anterior cingulate cortex. Note: the overlapped region in LMTG included 19 voxels. Considering the previous findings about LMTG in consciousness, it was also included in the following analysis.

3.2. Intact degree centrality in REM-sleep

The above five regions identified (SMA, SACC, bilateral SMG, and LMTG) were used as ROIs in REM-sleep datasets to test whether their degree centrality would be significantly reduced during N3-sleep, and intact during REM-sleep. There were three regions (SACC, SMA and LMTG) that showed a significant reduction of degree centrality during N3-sleep compared with REM-sleep and awake state. Both LSMG and RSMG showed significantly reduced degree centrality during N3-sleep compared with REM-sleep, and this difference was marginally significant between N3-sleep and awake (Fig. 3). We also validated the above findings by performing degree centrality analysis with different edge thresholds ($r > 0.2$ and $r > 0.4$) (Dai et al., 2015). Our results showed that all findings remained consistent when using different thresholds (Supplementary fig. 3).

3.3. ROI-based functional connectivity during consciousness

To reveal the connectivity of each pair of regions among the five brain regions, ROI-based functional connectivity was performed for all the states in the four groups. The results showed that each pair of regions (among the five brain regions) within each group had a significantly positive functional connectivity during consciousness or awake-state. Furthermore, the correlations of the strengths of the functional connectivity, i.e. the z-values obtained from the previous steps, are significant between each pair of groups during consciousness or awake-states (Fig. 4 and Supplementary fig. 4). These results indicated that the functional connectivity within these five brain regions were stable across different conscious states. For the functional connectivity values among the five regions in reduced consciousness and unconsciousness, please see Supplementary fig. 5

3.4. The relationship between functional connectivity and levels of consciousness

The mean functional connectivity z-value among the five regions was significantly correlated with levels of consciousness states in the sleep group ($\rho = 0.67$, $p < 0.01$), DOC group ($\rho = 0.79$, $p < 0.01$), and REM-sleep group ($\rho = 0.48$, $p < 0.01$). Similar as the mean strength of functional connectivity, if the functional connectivity with a z-value (> 0.3095) was regarded as an edge, the total edge number among the five brain regions also showed a significant correlation in the sleep group ($\rho = 0.67$, $p < 0.01$), DOC group ($\rho = 0.81$, $p < 0.01$), and REM-sleep group ($\rho = 0.59$, $p < 0.01$) (Fig. 5). All the above p values were FDR corrected.

3.5. Specific functional connectivity which reduced during unconscious states

Comparing the functional connectivity of each pair of regions between consciousness and unconsciousness states, the functional connectivity between SMA and bilateral SMG, the functional connectivity between SACC and LSMG, the functional connectivity between SACC and LMTG, as well as the functional connectivity between bilateral SMG, showed a significant reduction in the unconsciousness state for all groups (Fig. 6). This result was further confirmed by voxel-wise analysis using the five ROIs (SMA, SACC, bilateral SMG and LMTG) as seeds (Fig. 7). Additionally, within the above the functional connectivity with

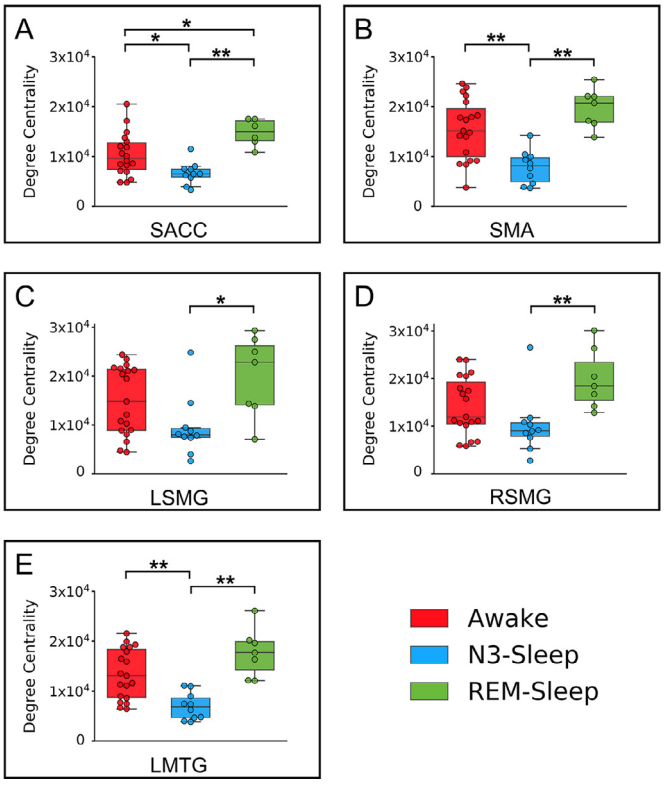

Fig. 3. Degree centrality in REM-sleep group. The degree centrality (DC) values for awake, REM-sleep and N3-sleep states in SMA, SACC, LSMG, RSMG, and LMTG. (A) SACC: H(2) = 13.86, $\eta_H^2 = 0.38$, $p < 0.001$; post-hoc test showed N3-sleep < REM-sleep, $p < 0.001$, and N3-sleep < awake, $p = 0.012$. (B) SMA: H(2) = 13.79, $\eta_H^2 = 0.36$, $p = 0.001$; post-hoc test showed N3-sleep < REM-sleep, $p < 0.001$, and N3-sleep < awake, $p = 0.002$. (C) LSMG: H(2) = 7.32, $\eta_H^2 = 0.16$, $p = 0.026$; post-hoc test showed N3-sleep < REM-sleep, $p = 0.012$, and N3-sleep < awake, $p = 0.072$. (D) RSMG: H(2) = 8.89, $\eta_H^2 = 0.21$, $p = 0.012$; post-hoc test showed N3-sleep < REM-sleep, $p = 0.005$, and N3-sleep < awake, $p = 0.070$. (E) LMTG:H(2) = 16.65, $\eta_H^2 = 0.44$, $p < 0.001$; post-hoc test showed N3-sleep < REM-sleep, $p < 0.001$, and N3-sleep < awake, $p < 0.001$. * means $p < 0.05$ FDR corrected. ** means $p < 0.01$ FDR corrected.

significant reduction during unconsciousness, the functional connectivity between SACC and LSMG, the functional connectivity between SACC and LMTG, as well as the functional connectivity between bilateral SMG, were significantly reduced in MCS compared with BI in the DOC group. But there was no functional connectivity which showed significant reduction in the N1-sleep or REM-sleep compared with awake state (Supplementary Fig. 6).

4. Discussion

In this study, we employed a graph-theoretical measure, i.e., degree centrality, and functional connectivity analysis to investigate the hubs in the brain's resting state that support consciousness. Degree centrality reflects the connections of one node with all other nodes throughout the brain. Our results revealed a reduced degree centrality in SMA, SACC, bilateral SMG and LMTG in the unconscious states (N3-sleep, anesthesia, and UWS) compared with the conscious and altered/partially conscious states (N1-sleep, MCS and REM-sleep).

Furthermore, functional connectivity analysis demonstrated that the connections among these five regions were significantly reduced during these unconscious states. Most interestingly, we found that this higher-order sensorimotor integration circuit was fully present in the REM-sleep, showing no difference compared with the awake states while exhibiting significant difference compared with the N3-sleep. This reduces sensory and motor input processing (as both are minimum in REM-sleep) as possible confounds of the higher-order sensorimotor integration circuit involved in the neural processing supporting consciousness. Therefore, we conclude that regions forming a higher-order sensorimotor integration circuit are involved in supporting consciousness through their role as hubs within the brain's global functional network.

During the REM-sleep, one loses the ability of movement and sensory inputs from the external world. Most interestingly, similar as the REM-sleep, one type of patients named as cognitive motor dissociation (CMD) (Schiff, 2015), shows signs of consciousness with command-following brain activation but no detectable behavioral response (Monti et al., 2010). In the previous literature, using motor imagery tasks, task-related activation in SMA can be used to identify CMD patients (Owen et al., 2006). However, the difficulty of such tasks and the cooperation of patients could lead to false negatives in the detection of CMD (Pan et al., 2020). Although the brain computer interface (BCI) provides another way to detect the CMD patients using face detection tasks (Pan et al., 2020), the current results may provide a much easier way to identify the CMD patients by using resting-state fMRI dataset without including any active tasks. More importantly, given that most patients with DOC had serious brain injuries and structural distortion, the ROI-based functional connectivity method should have more clinical potential compared with the voxel-wise degree centrality analysis.

Furthermore, previous studies demonstrated global changes of degree centrality during unconsciousness (Hashmi et al., 2017; Tagliazucchi et al., 2013b). Our results extend these findings by showing significantly decreased degree centrality in specific brain regions: the SMA, SACC, bilateral SMG, LMTG in the unconscious states compared with the conscious and altered conscious states across all groups. All these five regions exhibited high degree centrality in the healthy conscious brain in previous studies (van den Heuvel and Sporns, 2013). Regions with high degree centrality enable efficient communication, and therefore information integration in a global way (van den Heuvel and Sporns, 2013). Consequently, the reduction in the degree centrality in these regions during unconsciousness possibly indicates their role in supporting consciousness within the brain's global functional network.

Our findings on the relationship between SMA and conscious processing are supported by previous studies in both fully conscious and unconscious subjects. The SMA has been shown to be involved in conscious processing in a variety of different tasks requiring sensorimotor integration. For instance, one study found that suppressing brain activity in the SMA affected visual perception (Martin-Signes et al., 2019). Using the subject's own name as stimulus, MCS patients showed stronger SMA response to their own names than UWS patients (Qin et al., 2010). SACC is another region involved in motor initiation, in which damages can result in akinetic mutism (Boly et al., 2017). SACC is also a core region of the salience network (Seeley et al., 2007), which shows altered activation during anesthesia (Huang et al., 2014), sleep (Mitra et al., 2015), and brain injury (Mitra et al., 2015; Qin et al., 2015). Our previous study showed the functional connectivity between the SACC and insula was correlated with the consciousness levels in DOC patients (Qin et al., 2015). This was consistent with the voxel-wise functional connectivity in the current study (Fig. 7).

Beside these motor regions, the SMG, a higher-order sensory region, showed a significant reduction of global integration during unconsciousness (Luppi et al., 2019). More importantly, the SMG is part of the inferior parietal lobule (IPL) which was reported to show reduced brain activation in the unconscious states (Lichtner et al., 2018). Since the IPL is close to the temporal and occipital cortices and receives both auditory and visual information (Dehaene and Changeux, 2011), and is involved in heartbeat awareness and body-centered perception (e.g., face and body) (Blanke et al., 2015), it is suggested to play a central role in integrating external and internal sensory information. Similar as the SMG, the LMTG was regarded as a part of the temporo-parietal-occipital hot zone, and was more related to content-specific neural correlates of consciousness in previous studies (Koch et al., 2016). Further-

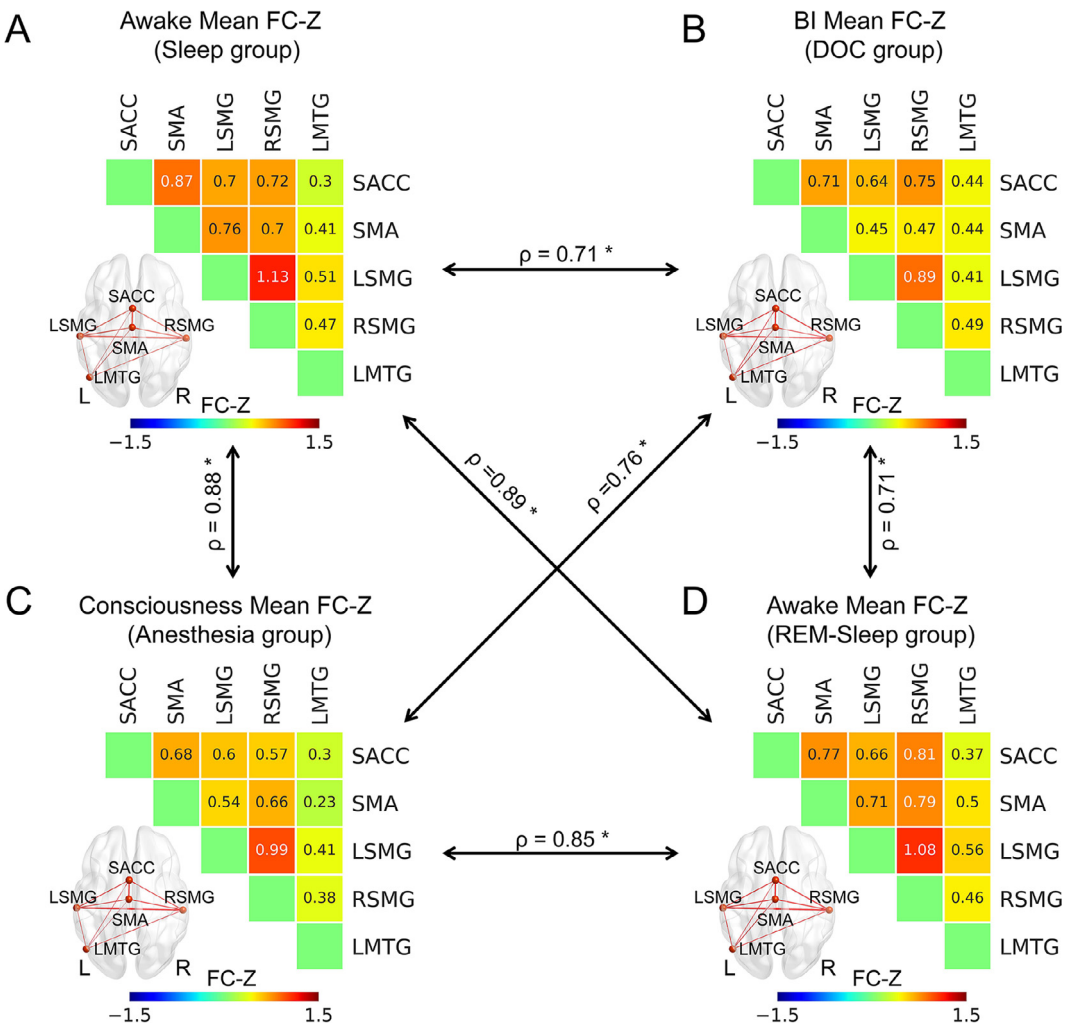

Fig. 4. ROI-based functional connectivity during consciousness in all four groups. (A) z-values for the awake-state in the sleep group; (B) z-values for the BI patients in the DOC group; (C) z-values for the conscious state in the anesthesia group;(D) z-values for the awake-states in the REM-sleep group. The black arrow represented the correlation of the corresponding functional connectivity pairs between two groups, which was calculated with the Spearman's correlation. * means $p < 0.05$ FDR corrected. The thickness of lines in brain image represented the functional connectivity z-values between two states.

more, the LMTG was also involved in the visual word detection task (Dehaene et al., 2001), and showed more activation during dreaming experience compared with no dreaming (Siclari et al., 2017).

More interestingly, the current results showed that the sum of functional connectivity among these five regions was correlated with the levels of consciousness. This suggests that they could form a circuit within the brain's global functional network, in which higher-order sensorimotor information integration may play an important role in supporting consciousness. Previous brain imaging literature about propofol-induced (Mashour and Hudetz, 2018) and sevoflurane-iduced anesthesia (Palanca et al., 2017) mostly emphasized reduced connectivity in the default-mode network, frontoparietal network, as well as thalamo-cortical connections (Guldenmund et al., 2016; Huang et al., 2020; Jordan et al., 2013; Luppi et al., 2019; Palanca et al., 2015; Qiu et al., 2017), while a few studies highlighted the role of pallido-cortical connectivity in supporting consciousness (Crone et al., 2017), or salience network (Guldenmund et al., 2013). Similarly, previous sleep studies also focused on the frontoparietal network, default-mode network and thalamo-cortical connection based on comparisons between the awake state and N3-sleep (Chow et al., 2013; Horovitz et al., 2009; Spoormaker et al., 2012; Wilson et al., 2015). Combining sleep, anesthesia and DOC patients, the current results highlighted the role of higher-order sensorimotor integration in supporting consciousness, which has been previously implicated by studies on propofol-induced anesthesia (Lichtner et al., 2018), N3-sleep (Mitra et al., 2015), and DOC patients (Demertzi et al., 2015), but not explicitly emphasized.

Furthermore, the relationship between higher-order sensorimotor integration and consciousness was supported by a recent study which indicated that the auditory-visual information could be used to differentiate MCS from UWS patients, and might be required for conscious perception (Demertzi et al., 2015). The current results extended these previous findings by showing further information integration between multi-sensory information integration with motor information. This is supported by the result that this higher-order sensorimotor information integration circuit was present during REM-sleep where one has vivid conscious experience with minimum sensory input and motor production (Chow et al., 2013). Taken together, the current results indicated that higher-order sensorimotor information integration may be essential for conscious perception, and might be one crucial part of the neural mechanisms mediating consciousness.

Following a recent assumption (Aru et al., 2012), neural prerequisites of consciousness (NCCpre) must be distinguished from the neural correlates of consciousness (NCC proper). The NCCpre refers to those neural conditions that enable actual consciousness; they may refer to the necessary but not yet sufficient conditions of actual consciousness; a typical example is the changes in the internal prestimulus activity level

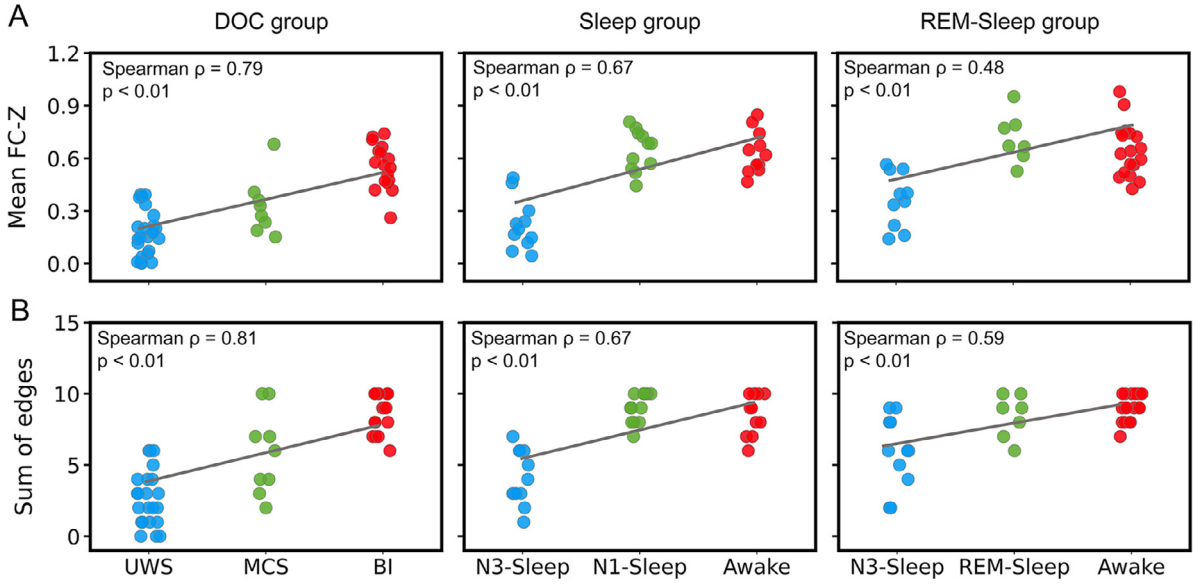

Fig. 5. The relationship between functional connectivity and levels of consciousness. (A) The correlation between mean functional connectivity (FC) z-values (of all FCs among the five ROIs: SACC, SMA, LSMG, RSMG and LMTG) for each subject and consciousness states, in patients with DOC (left panel), sleep group (middle panel), and REM-sleep group (right panel). (B) The correlation between the sum of edges (of all FCs among the five ROIs: SACC, SMA, LSMG, RSMG and LMTG) and consciousness states, in patients with DOC (left panel), sleep group (middle panel), and REM-sleep group (right panel). Edge = one FC with Z value > 0.3095.

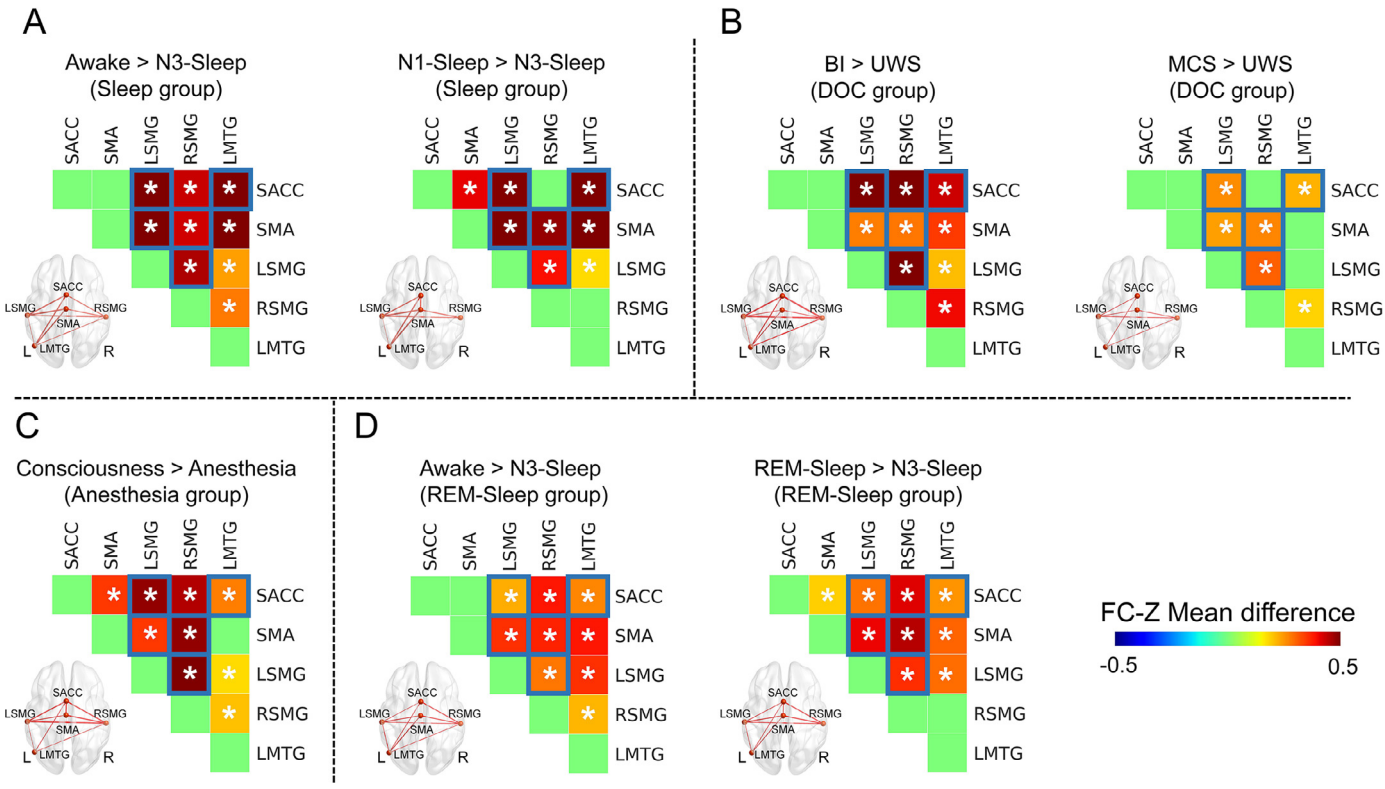

Fig. 6. Reduced functional connectivity during unconsciousness. (A) Functional connectivity (FC) with significant reduction in the N3-sleep compared with awake and N1-sleep in the sleep group. (B) FC with a significant reduction in UWS compared with BI and MCS in the DOC group. (C) FC with a significant reduction in anesthesia compared with consciousness in the anesthesia group. (D) FC with significant reduction in N3-sleep compared with awake and REM-sleep in the REM-sleep group. * means $p < 0.05$, FDR corrected. The functional connectivity marked with blue squares showed consistent reduction during unconsciousness in all four groups. The thickness of lines in brain image represented the difference of functional connectivity between two states.

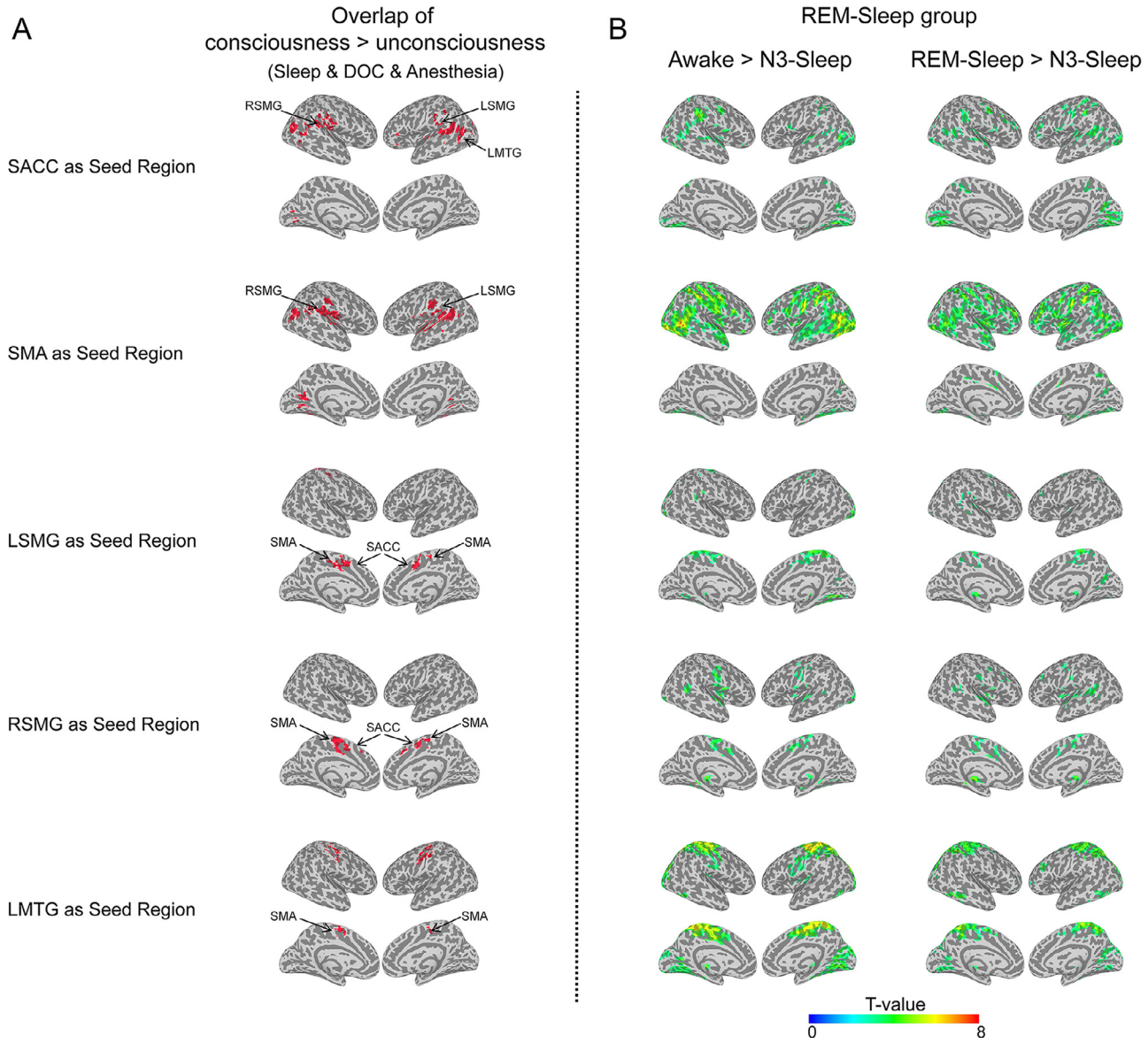

Fig. 7. Voxel-wise functional connectivity in unconscious states. (A) For each seed region, the overlapped regions for all consciousness vs. unconsciousness contrasts (BI > UWS; MCS > UWS, awake > N3-sleep, N1-sleep > N3-sleep, and consciousness > anesthesia) (volume > 20 voxels). (B) In REM-sleep group, the voxel-wise FC contrasts: Awake > N3-sleep (the left panel) and REM-sleep > N3-sleep. The activation clusters are displayed ($p < 0.005$ uncorrected, volume > 20 voxels).

that can predict subsequent consciousness in the presence of an actual external stimulus (see (Northoff and Lamme, 2020) for extensive discussion of pre-stimulus findings). However, in the absence of an external stimulus, the pre-stimulus changes do not amount to consciousness by themselves; they may thus be necessary but not sufficient for actual consciousness. Yet another important dimension is the one of neural predisposition of consciousness (NPC) as introduced by (Northoff, 2013). The NPC refers to the neural capacity for consciousness, i.e., its predisposition, that is, whether it is in principle possible to elicit consciousness in a brain. Hence, the NPC refers to the necessary neural condition of possible (rather than actual) consciousness; this distinguishes the NPC from both NCC proper and NCCpre that refer to actual (rather than possible) consciousness.

Which conditions are referred to in the current paper? As we here only describe changes in the resting state, we assume that they refer to the NPC: a brain must display connectivity pattern in higher-order sensorimotor circuits to exhibit possible consciousness. This allows higher-order sensorimotor integration which may be key for integrating the various inputs from different sensory modalities. We thus consider the present result of higher-order sensorimotor circuit in conjunction with a recent study that provides evidence that input processing is a key capacity for consciousness (Zilio et al., 2021). As we did not include task state nor specific contents of consciousness, we cannot clearly distinguish whether higher-order sensorimotor connectivity and integration is a true NPC or, alternatively, an NCCpre, a neural prerequisite that enables the actual consciousness. What is clear is that our findings do not refer to the NCC proper as for that we would have required to probe task-evoked activity in both conscious and unconscious states.

In the current study, the Default-mode network also showed reduced degree centrality in several contrasts between the conscious/altered conscious and unconscious states, such as the UWS (compared with MCS), as well as the anesthesia (compared with consciousness in anesthesia group), but not in all the contrasts between conscious/altered and unconscious states (Fig. 2). This was consistent with the previous

studies. For instance, one study showed that the functional connectivity was correlated with levels of consciousness (Vanhaudenhuyse et al., 2010), while another study indicated that default-mode network was related to the recovery of consciousness, not the levels of consciousness (Norton et al., 2012).

Similar as the default-mode network, the thalamus also showed no commonly reduced degree centrality among the unconsciousness states except in UWS compared with MCS, and in anesthesia compared with consciousness state. Considering the relationship between the thalamus and arousal, and the broad connection between the thalamus and the cortex (Aru et al., 2019), we also tested the functional connectivity between the thalamus and the five ROIs. None of these functional connectivity showed consistent reduction during unconsciousness among the four groups (sleep, anesthesia, DOC and REM-sleep) (Supplementary figure 7). Specifically, the thalamus had significantly reduced functional connectivity with the SACC, SMA, and bilateral SMG during anesthesia compared with consciousness state, whereas these differences were not seen in N3-sleep compared with awake state. These results may indicate one of the crucial differences between sleep and anesthesia, and explain why people could be woken up during sleep, but not during anesthesia. This assumption is supported by a recent study indicating that thalamus was involved in the sleep-awake transition (Gent et al., 2018), as well as a recent anesthesia study that stimulation on thalamus could effectively restore arousal and wake-like neural processing in macaques (Redinbaugh et al., 2020). In conclusion, the results from present study and previous literature about thalamus and consciousness indicated that the role of the thalamus-cortex connection in consciousness needs further investigation in the future.

Another brain region worth mentioning is the visual cortex, which showed reduced degree centrality in the contrasts between consciousness and unconsciousness states in both the sleep group and anesthesia group, but not in the contrast between BI and UWS. This finding is in line with previous consciousness studies, where visual cortex showed reduced connection with the posterior cingulate cortex during anesthesia (Amico et al., 2014), and reduced connection with the auditory cortex in UWS compared with MCS (Demertzi et al., 2015). Additionally, the current results showed that the visual cortex had reduced functional connectivity with both SACC and SMA during N3-sleep compared with REM-sleep. Considering the limited visual input in the current experimental conditions (participants being required to keep their eyes closed during consciousness states), the higher functional connectivity between the visual cortex and other brain regions during consciousness states may be due to top-down influences. One previous study had shown similar top-down connection with an EEG oddball design, which could be used to differentiate UWS from MCS (Boly et al., 2011). However, the visual cortex showed no difference in degree centrality between UWS and BI patients in the current study. This was also supported by previous studies that showed preserved connectivity within the visual network (Sinitsyn et al., 2018), or between the visual and default-mode network (Di Perri et al., 2018) during unconsciousness. This suggests that the relationship between the visual cortex and consciousness requires further investigation in the future.

Given that some of the anesthetic effects on the BOLD signal could be physiological in nature, and hence unrelated to unconsciousness (Huang et al., 2020), in the current study, 17 participants of propofol-induced anesthesia and 6 participants of sevoflurane-induced anesthesia were included. In order to compare the difference between these two anesthetic agents, a two-way ANOVA was performed, where the anesthetic agent drug and consciousness level were considered as two independent variables. Within all the ROIs, we found no significant main effects of drug, but a significant main effect of consciousness level, as well as a significant interaction effect between anesthetic agent and consciousness in SACC ($p = 0.035$ FDR corrected, but not the other four, i.e. SMA, LSMG, RSMG, and LMTG). For the propofol-induced anesthesia, there was a significant reduction in the degree centrality in all five ROIs during unconsciousness ($p < 0.05$ FDR corrected). For the sevoflurane-induced anesthesia, the results also showed similar trends (See Supplementary fig. 8). These results suggest that there are no major differences of degree centrality between the two drugs. In the future, it may be useful to test other anesthetic drugs (e.g., ketamine) to confirm the current results.

Several issues should be noted. The first issue is that we did not specifically investigate dreams during both NREM and REM but took REM-sleep simply as an index of the presence of consciousness (Windt et al., 2016). Although different from wakefulness, the REM-sleep is considered a particular form of environmentally "disconnected" consciousness state (Tagliazucchi et al., 2013a). Here we not only showed the similarity of functional connectivity of the five brain hubs between a presumed dream state, i.e., REM, and the fully awake conscious state, but also its difference from that in the N3-sleep. Secondly, the sample size of each individual state in the current study is limited. However, when combined for the consciousness or unconsciousness conditions, the sample size is actually satisfactory. For instance, for the sleep groups (we have a sleep group and an independent REM-sleep group) 31 subjects constituted the consciousness condition (with 12 in the awake state from the sleep group and 19 from the REM-sleep group), and 23 subjects constituted the unconsciousness condition (i.e. the N3-sleep state, with 12 from the sleep-group and 11 from REM-sleep group). Similarly, for the DOC patients, 27 patients constituted the consciousness condition (with 18 from the BI and 9 from the MCS), and 23 patients constituted the unconsciousness condition (the UWS). Hence, the sample sizes for the comparison of consciousness vs. unconsciousness for anesthesia, sleep and DOC respectively, are actually not too small, and sufficiently balanced ($N>20$). We performed the statistical analysis for these contrasts, and obtained similar results as those shown in Fig. 2 (see supplementary figure 9). Considering that various higher cognitive function difference other than consciousness/unconsciousness may confound the comparisons of the different groups, collapsing datasets from different states in different groups may minimize these confounding effects, and help focus on the possible brain regions for consciousness. In fact, the consistence between the two analyses indicated that the current results were reliable. Even so, further confirmation from future studies is still necessary.

5. Conclusions

In summary, we demonstrated that the SMA, SACC, bilateral SMG and LMTG participate in forming a higher-order sensorimotor integration circuit within the brain's global functional network that supports consciousness. All these regions showed significant decreases in degree centrality and functional connectivity with each other during different unconscious conditions, i.e., anesthesia, N3-sleep, and patients with UWS. Furthermore, the mean strength and edge of functional connectivity of the five regions were significantly correlated with levels of consciousness. Interestingly, these properties were unchanged between wakefulness and REM-sleep. Based on their known functions in movement initiation and sensory information processing, we conclude that these regions could form a higher-order sensorimotor integration circuit that is essential for maintaining consciousness.

Data and materials availability

All data needed to evaluate the conclusions in the paper are present in the paper and the Supplementary Materials. Additional data related to this paper may be requested from the corresponding author.

Declaration of Competing Interest

None declared.

Credit authorship contribution statement

Pengmin Qin: Conceptualization, Methodology, Formal analysis, Data curtion, Writing – original draft, Writing – review & editing, Visualization, Project administration, Funding acquisition. **Xuehai Wu:** Conceptualization, Methodology, Investigation, Writing – review & editing, Funding acquisition. **Changwei Wu:** Investigation. **Hang Wu:** Software, Formal analysis, Visualization. **Jun Zhang:** Investigation. **Zirui Huang:** Investigation. **Xuchu Weng:** Conceptualization. **Di Zang:** Writing – original draft. **Zengxin Qi:** Investigation. **Weijun Tang:** Investigation. **Tanikawa Hiromi:** Investigation. **Jiaxing Tan:** Investigation. **Sean Tanabe:** Investigation. **Stuart Fogel:** Investigation, Writing – original draft. **Anthony G. Hudetz:** Writing – original draft. **Yihong Yang:** Writing – original draft. **Emmanuel A Stamatakis:** Writing – original draft. **Ying Mao:** Conceptualization, Methodology, Writing – review & editing, Supervision. **Georg Northoff:** Conceptualization, Methodology, Writing – original draft, Writing – review & editing, Supervision, Funding acquisition.

Acknowledgments

This work was sponsored by grants from Key Realm R&D Program of Guangzhou (202007030005 to PQ), the National Natural Science Foundation of China (Grant 31971032, 31771249 to PQ; Grants 81571025 to XW), International Cooperation Project from Shanghai Science Foundation (No.18410711300 to Xuehai Wu), Shanghai Science and Technology Development funds (No. 16JC1420100 to Y.M), Shanghai Municipal Science and Technology Major Project (No.2018SHZDZX01 to Y.M), Natural Science Foundation and Major Basic Research Program of Shanghai (16JC1420100), Ministry of Science and Technology in Taiwan (MOST 105-2628-B-038-013-MY3), National Science Foundation of China (31471072), Taiwan Ministry of Science and Technology (105-2410-H-038-006-MY3, 105-2410-H-038-005-MY2); and Taipei Medical University (104-6402-006-110), and National Institute of General Medical Sciences of the National Institutes of Health (R01-GM103894, to AGH), Canadian Institutes of Health Research (CIHR), Michael Smith Foundation (EJLB-CIHR), The Hope for Depression Research Foundation (HDRF). This research project was also supported by the HBP Joint Platform to GN, funded from the European Union's Horizon 2020 Framework Program for research and Innovation under the specific Grant Agreement No 785907 (Human Brian Project SGA 2).

Supplementary materials

Supplementary material associated with this article can be found, in the online version, at doi:10.1016/j.neuroimage.2021.117850.

References

Amico, E., Gomez, F., Di Perri, C., Vanhaudenhuyse, A., Lesenfants, D., Boveroux, P., Bonhomme, V., Brichant, J.F., Marinazzo, D., Laureys, S., 2014. Posterior cingulate cortex-related co-activation patterns: a resting state FMRI study in propofol-induced loss of consciousness. PLoS One 9, e100012.

Amico, E., Marinazzo, D., Di Perri, C., Heine, L., Annen, J., Martial, C., Dzemidzic, M., Kirsch, M., Bonhomme, V., Laureys, S., Goñi, J., 2017. Mapping the functional connectome traits of levels of consciousness. Neuroimage 148, 201–211.

Aru, J., Bachmann, T., Singer, W., Melloni, L., 2012. Distilling the neural correlates of consciousness. Neurosci. Biobehav. Rev. 36, 737–746.

Aru, J., Suzuki, M., Rutiku, R., Larkum, M.E., Bachmann, T., 2019. Coupling the state and contents of consciousness. Front. Syst. Neurosci. 13, 43.

Bachmann, T., 2015. On the brain-imaging markers of neural correlates of consciousness. Front. Psychol. 6, 868.

Blanke, O., Slater, M., Serino, A., 2015. Behavioral, neural, and computational principles of bodily self-consciousness. Neuron 88, 145–166.

Boly, M., Garrido, M.I., Gosseries, O., Bruno, M.A., Boveroux, P., Schnakers, C., Massimini, M., Litvak, V., Laureys, S., Friston, K., 2011. Preserved feedforward but impaired top-down processes in the vegetative state. Science 332, 858–862.

Boly, M., Massimini, M., Tsuchiya, N., Postle, B.R., Koch, C., Tononi, G., 2017. Are the neural correlates of consciousness in the front or in the back of the cerebral cortex? Clinical and neuroimaging evidence. J. Neurosci. 37, 9603–9613.

Bullmore, E., Sporns, O., 2012. The economy of brain network organization. Nat. Rev. Neurosci. 13, 336–349.

Casali, A.G., Gosseries, O., Rosanova, M., Boly, M., Sarasso, S., Casali, K.R., Casarotto, S., Bruno, M.A., Laureys, S., Tononi, G., Massimini, M., 2013. A theoretically based index of consciousness independent of sensory processing and behavior. Sci. Transl. Med. 5, 198ra105.

Chow, H.M., Horovitz, S.G., Carr, W.S., Picchioni, D., Coddington, N., Fukunaga, M., Xu, Y., Balkin, T.J., Duyn, J.H., Braun, A.R., 2013. Rhythmic alternating patterns of brain activity distinguish rapid eye movement sleep from other states of consciousness. Proc. Natl. Acad. Sci. U. S. A. 110, 10300–10305.

Crick, F., Koch, C., 2003. A framework for consciousness. Nat. Neurosci. 6, 119–126.

Crone, J.S., Lutkenhoff, E.S., Bio, B.J., Laureys, S., Monti, M.M., 2017. Testing proposed neuronal models of effective connectivity within the cortico-basal ganglia-thalamo–cortical loop during loss of consciousness. Cereb. Cortex 27, 2727–2738.

Dai, Z., Yan, C., Li, K., Wang, Z., Wang, J., Cao, M., Lin, Q., Shu, N., Xia, M., Bi, Y., He, Y., 2015. Identifying and mapping connectivity patterns of brain network hubs in Alzheimer's disease. Cereb. Cortex 25, 3723–3742.

Dehaene, S., Changeux, J.P., 2011. Experimental and theoretical approaches to conscious processing. Neuron 70, 200–227.

Dehaene, S., Naccache, L., Cohen, L., Bihan, D.L., Mangin, J.F., Poline, J.B., Riviere, D., 2001. Cerebral mechanisms of word masking and unconscious repetition priming. Nat. Neurosci. 4, 752–758.

Demertzi, A., Antonopoulos, G., Heine, L., Voss, H.U., Crone, J.S., de Los Angeles, C., Bahri, M.A., Di Perri, C., Vanhaudenhuyse, A., Charland-Verville, V., Kronbichler, M., Trinka, E., Phillips, C., Gomez, F., Tshibanda, L., Soddu, A., Schiff, N.D., Whitfield--Gabrieli, S., Laureys, S., 2015. Intrinsic functional connectivity differentiates minimally conscious from unresponsive patients. Brain 138, 2619–2631.

Demertzi, A., Tagliazucchi, E., Dehaene, S., Deco, G., Barttfeld, P., Raimondo, F., Martial, C., Fernandez-Espejo, D., Rohaut, B., Voss, H.U., Schiff, N.D., Owen, A.M., Laureys, S., Naccache, L., Sitt, J.D., 2019. Human consciousness is supported by dynamic complex patterns of brain signal coordination. Sci. Adv. 5, eaat7603.

Di, H.B., Yu, S.M., Weng, X.C., Laureys, S., Yu, D., Li, J.Q., Qin, P.M., Zhu, Y.H., Zhang, S.Z., Chen, Y.Z., 2007. Cerebral response to patient's own name in the vegetative and minimally conscious states. Neurology 68, 895–899.

Di Perri, C., Amico, E., Heine, L., Annen, J., Martial, C., Larroque, S.K., Soddu, A., Marinazzo, D., Laureys, S., 2018. Multifaceted brain networks reconfiguration in disorders of consciousness uncovered by co-activation patterns. Hum. Brain Mapp. 39, 89–103.

Engemann, D.A., Raimondo, F., King, J.R., Rohaut, B., Louppe, G., Faugeras, F., Annen, J., Cassol, H., Gosseries, O., Fernandez-Slezak, D., Laureys, S., Naccache, L., Dehaene, S., Sitt, J.D., 2018. Robust EEG-based cross-site and cross-protocol classification of states of consciousness. Brain 141, 3179–3192.

Fang, Z., Ray, L.B., Owen, A.M., Fogel, S.M., 2019. Brain activation time-locked to sleep spindles associated with human cognitive abilities. Front. Neurosci. 13, 46.

Gent, T.C., Bandarabadi, M., Herrera, C.G., Adamantidis, A.R., 2018. Thalamic dual control of sleep and wakefulness. Nat. Neurosci. 21, 974–984.

Giacino, J.T., Kalmar, K., Whyte, J., 2004. The JFK coma recovery scale-revised: measurement characteristics and diagnostic utility. Arch. Phys. Med. Rehabil. 85, 2020–2029.

Guldenmund, P., Demertzi, A., Boveroux, P., Boly, M., Vanhaudenhuyse, A., Bruno, M.A., Gosseries, O., Noirhomme, Q., Brichant, J.F., Bonhomme, V., Laureys, S., Soddu, A., 2013. Thalamus, brainstem and salience network connectivity changes during propofol-induced sedation and unconsciousness. Brain Connect. 3, 273–285.

Guldenmund, P., Gantner, I.S., Baquero, K., Das, T., Demertzi, A., Boveroux, P., Bonhomme, V., Vanhaudenhuyse, A., Bruno, M.A., Gosseries, O., Noirhomme, Q., Kirsch, M., Boly, M., Owen, A.M., Laureys, S., Gomez, F., Soddu, A., 2016. Propofol-induced frontal cortex disconnection: a study of resting-state networks, total brain connectivity, and mean BOLD signal oscillation frequencies. Brain Connect. 6, 225–237.

Hashmi, J.A., Loggia, M.L., Khan, S., Gao, L., Kim, J., Napadow, V., Brown, E.N., Akeju, O., 2017. Dexmedetomidine disrupts the local and global efficiencies of large-scale brain networks. Anesthesiology 126, 419–430.

Horovitz, S.G., Braun, A.R., Carr, W.S., Picchioni, D., Balkin, T.J., Fukunaga, M., Duyn, J.H., 2009. Decoupling of the brain's default mode network during deep sleep. Proc. Natl. Acad. Sci. U.S.A. 106, 11376–11381.

Houldin, E., Fang, Z., Ray, L.B., Owen, A.M., Fogel, S.M., 2019. Toward a complete taxonomy of resting state networks across wakefulness and sleep: an assessment of spatially distinct resting state networks using independent component analysis. Sleep 42.

Hu, X., Cheng, L.Y., Chiu, M.H., Paller, K.A., 2020. Promoting memory consolidation during sleep: a meta-analysis of targeted memory reactivation. Psychol. Bull. 146, 218–244.

Huang, Z., Liu, X., Mashour, G.A., Hudetz, A.G., 2018. Timescales of intrinsic BOLD signal dynamics and functional connectivity in pharmacologic and neuropathologic states of unconsciousness. J. Neurosci..

Huang, Z., Wang, Z., Zhang, J., Dai, R., Wu, J., Li, Y., Liang, W., Mao, Y., Yang, Z., Holland, G., Zhang, J., Northoff, G., 2014. Altered temporal variance and neural synchronization of spontaneous brain activity in anesthesia. Hum. Brain Mapp. 35, 5368–5378.

Huang, Z., Zhang, J., Wu, J., Mashour, G.A., Hudetz, A.G., 2020. Temporal circuit of macroscale dynamic brain activity supports human consciousness. Sci. Adv. 6 eaaz0087.

Huang, Z., Zhang, J., Wu, J., Qin, P., Wu, X., Wang, Z., Dai, R., Li, Y., Liang, W., Mao, Y., Yang, Z., Zhang, J., Wolff, A., Northoff, G., 2016. Decoupled temporal variability and signal synchronization of spontaneous brain activity in loss of consciousness: an fMRI study in anesthesia. Neuroimage 124, 693–703.

Jordan, D., Ilg, R., Riedl, V., Schorer, A., Grimberg, S., Neufang, S., Omerovic, A., Berger, S., Untergehrer, G., Preibisch, C., Schulz, E., Schuster, T., Schroter, M., Spoormaker, V., Zimmer, C., Hemmer, B., Wohlschlager, A., Kochs, E.F., Schneider, G., 2013. Simultaneous electroencephalographic and functional magnetic resonance imaging indicate impaired cortical top-down processing in association with anesthetic-induced unconsciousness. Anesthesiology 119, 1031–1042.

Katoh, T., Ikeda, K., 1998. The effects of fentanyl on sevoflurane requirements for loss of consciousness and skin incision. Anesthesiology 88, 18–24.
Kertai, M.D., Whitlock, E.L., Avidan, M.S., 2012. Brain monitoring with electroencephalography and the electroencephalogram-derived bispectral index during cardiac surgery. Anesth. Analg. 114, 533–546.
Koch, C., Massimini, M., Boly, M., Tononi, G., 2016. Neural correlates of consciousness: progress and problems. Nat. Rev. Neurosci. 17, 307–321.
Larson-Prior, L.J., Zempel, J.M., Nolan, T.S., Prior, F.W., Snyder, A.Z., Raichle, M.E., 2009. Cortical network functional connectivity in the descent to sleep. Proc. Natl. Acad. Sci. U.S.A. 106, 4489–4494.
Laureys, S., 2005. The neural correlate of (un)awareness: lessons from the vegetative state. Trends Cognit. Sci. 9, 556–559.
Lichtner, G., Auksztulewicz, R., Kirilina, E., Velten, H., Mavrodis, D., Scheel, M., Blankenburg, F., von Dincklage, F., 2018. Effects of propofol anesthesia on the processing of noxious stimuli in the spinal cord and the brain. Neuroimage 172, 642–653.
Liu, X., Lauer, K.K., Douglas Ward, B., Roberts, C., Liu, S., Gollapudy, S., Rohloff, R., Gross, W., Chen, G., Xu, Z., Binder, J.R., Li, S.J., Hudetz, A.G., 2017. Propofol attenuates low-frequency fluctuations of resting-state fMRI BOLD signal in the anterior frontal cortex upon loss of consciousness. Neuroimage 147, 295–301.
Luppi, A.I., Craig, M.M., Pappas, I., Finoia, P., Williams, G.B., Allanson, J., Pickard, J.D., Owen, A.M., Naci, L., Menon, D.K., Stamatakis, E.A., 2019. Consciousness-specific dynamic interactions of brain integration and functional diversity. Nat. Commun. 10, 4616.
Martin-Signes, M., Perez-Serrano, C., Chica, A.B., 2019. Causal contributions of the SMA to alertness and consciousness interactions. Cereb. Cortex 29, 648–656.
Martínez, D.E., Rudas, J., Demertzi, A., Charland-Verville, V., Soddu, A., Laureys, S., Gómez, F., 2020. Reconfiguration of large-scale functional connectivity in patients with disorders of consciousness. Brain Behav. 10, e1476.
Mashour, G.A., Hudetz, A.G., 2018. Neural correlates of unconsciousness in large-scale brain networks. Trends Neurosci. 41, 150–160.
Mitra, A., Snyder, A.Z., Tagliazucchi, E., Laufs, H., Raichle, M.E., 2015. Propagated infra-slow intrinsic brain activity reorganizes across wake and slow wave sleep. Elife 4.
Monti, M.M., Lutkenhoff, E.S., Rubinov, M., Boveroux, P., Vanhaudenhuyse, A., Gosseries, O., Bruno, M.A., Noirhomme, Q., Boly, M., Laureys, S., 2013. Dynamic change of global and local information processing in propofol-induced loss and recovery of consciousness. PLoS Comput. Biol. 9, e1003271.
Monti, M.M., Vanhaudenhuyse, A., Coleman, M.R., Boly, M., Pickard, J.D., Tshibanda, L., Owen, A.M., Laureys, S., 2010. Willful modulation of brain activity in disorders of consciousness. N. Engl. J. Med. 362, 579–589.
Moon, J.Y., Lee, U., Blain-Moraes, S., Mashour, G.A., 2015. General relationship of global topology, local dynamics, and directionality in large-scale brain networks. PLoS Comput. Biol. 11, e1004225.
Northoff, G., 2013. What the brain's intrinsic activity can tell us about consciousness? A tri-dimensional view. Neurosci. Biobehav. Rev. 37, 726–738.
Northoff, G., 2014. Do cortical midline variability and low frequency fluctuations mediate William James' "Stream of Consciousness"? "Neurophenomenal balance hypothesis" of "Inner time consciousness". Conscious. Cognit. 30, 184–200.
Northoff, G., Lamme, V., 2020. Neural signs and mechanisms of consciousness: is there a potential convergence of theories of consciousness in sight? Neurosci. Biobehav. Rev. 118, 568–587.
Norton, L., Hutchison, R.M., Young, G.B., Lee, D.H., Sharpe, M.D., Mirsattari, S.M., 2012. Disruptions of functional connectivity in the default mode network of comatose patients. Neurology 78, 175–181.
O'Regan, J.K., Noe, A., 2001. A sensorimotor account of vision and visual consciousness. Behav. Brain Sci. 24, 939–973 discussion 973-1031.
Owen, A.M., Coleman, M.R., Boly, M., Davis, M.H., Laureys, S., Pickard, J.D., 2006. Detecting awareness in the vegetative state. Science 313, 1402.
Palanca, B., Avidan, M.S., Mashour, G.A., 2017. Human neural correlates of sevoflurane-induced unconsciousness. Br. J. Anaesth. 119, 573–582.
Palanca, B.J., Mitra, A., Larson-Prior, L., Snyder, A.Z., Avidan, M.S., Raichle, M.E., 2015. Resting-state functional magnetic resonance imaging correlates of sevoflurane-induced unconsciousness. Anesthesiology 123, 346–356.
Pan, J., Xie, Q., Qin, P., Chen, Y., He, Y., Huang, H., Wang, F., Ni, X., Cichocki, A., Yu, R., Li, Y., 2020. Prognosis for patients with cognitive motor dissociation identified by brain-computer interface. Brain 143, 1177–1189.
Power, J.D., Barnes, K.A., Snyder, A.Z., Schlaggar, B.L., Petersen, S.E., 2012. Spurious but systematic correlations in functional connectivity MRI networks arise from subject motion. Neuroimage 59, 2142–2154.
Qin, P., Di, H., Liu, Y., Yu, S., Gong, Q., Duncan, N., Weng, X., Laureys, S., Northoff, G., 2010. Anterior cingulate activity and the self in disorders of consciousness. Hum. Brain Mapp. 31, 1993–2002.
Qin, P., Wu, X., Huang, Z., Duncan, N.W., Tang, W., Wolff, A., Hu, J., Gao, L., Jin, Y., Wu, X., Zhang, J., Lu, L., Wu, C., Qu, X., Mao, Y., Weng, X., Zhang, J., Northoff, G., 2015. How are different neural networks related to consciousness? Ann. Neurol. 78, 594–605.
Qiu, M., Scheinost, D., Ramani, R., Constable, R.T., 2017. Multi-modal analysis of functional connectivity and cerebral blood flow reveals shared and unique effects of propofol in large-scale brain networks. Neuroimage 148, 130–140.
Redinbaugh, M.J., Phillips, J.M., Kambi, N.A., Mohanta, S., Andryk, S., Dooley, G.L., Afrasiabi, M., Raz, A., Saalmann, Y.B., 2020. Thalamus modulates consciousness via layer-specific control of cortex. Neuron 106, 66–75.
Schiff, N.D., 2015. Cognitive motor dissociation following severe brain injuries. JAMA Neurol. 72, 1413–1415.
Seeley, W.W., Menon, V., Schatzberg, A.F., Keller, J., Glover, G.H., Kenna, H., Reiss, A.L., Greicius, M.D., 2007. Dissociable intrinsic connectivity networks for salience processing and executive control. J. Neurosci. 27, 2349–2356.
Siclari, F., Baird, B., Perogamvros, L., Bernardi, G., LaRocque, J.J., Riedner, B., Boly, M., Postle, B.R., Tononi, G., 2017. The neural correlates of dreaming. Nat. Neurosci. 20, 872–878.
Sinitsyn, D.O., Legostaeva, L.A., Kremneva, E.I., Morozova, S.N., Poydasheva, A.G., Mochalova, E.G., Chervyakova, O.G., Ryabinkina, J.V., Suponeva, N.A., Piradov, M.A., 2018. Degrees of functional connectome abnormality in disorders of consciousness. Hum. Brain Mapp. 39, 2929–2940.
Spoormaker, V., Gleiser, P., Czisch, M., 2012. Frontoparietal connectivity and hierarchical structure of the brain's functional network during. Sleep Front. Neurol. 3, 80.
Stender, J., Gosseries, O., Bruno, M.A., Charland-Verville, V., Vanhaudenhuyse, A., Demertzi, A., Chatelle, C., Thonnard, M., Thibaut, A., Heine, L., Soddu, A., Boly, M., Schnakers, C., Gjedde, A., Laureys, S., 2014. Diagnostic precision of PET imaging and functional MRI in disorders of consciousness: a clinical validation study. Lancet 384, 514–522.
Tagliazucchi, E., Behrens, M., Laufs, H., 2013a. Sleep neuroimaging and models of consciousness. Front. Psychol. 4, 256.
Tagliazucchi, E., von Wegner, F., Morzelewski, A., Brodbeck, V., Borisov, S., Jahnke, K., Laufs, H., 2013b. Large-scale brain functional modularity is reflected in slow electroencephalographic rhythms across the human non-rapid eye movement sleep cycle. Neuroimage 70, 327–339.
Tanabe, S., Huang, Z., Zhang, J., Chen, Y., Fogel, S., Doyon, J., Wu, J., Xu, J., Zhang, J., Qin, P., Wu, X., Mao, Y., Mashour, G.A., Hudetz, A.G., Northoff, G., 2020. Altered global brain signal during physiologic, pharmacologic, and pathologic states of unconsciousness in humans and rats. Anesthesiology 132, 1392–1406.
Tang, W., Liu, H., Douw, L., Kramer, M.A., Eden, U.T., Hamalainen, M.S., Stufflebeam, S.M., 2017. Dynamic connectivity modulates local activity in the core regions of the default-mode network. Proc. Natl. Acad. Sci. U.S.A. 114, 9713–9718.
Tononi, G., Boly, M., Massimini, M., Koch, C., 2016. Integrated information theory: from consciousness to its physical substrate. Nat. Rev. Neurosci. 17, 450–461.
Tsai, P.J., Chen, S.C., Hsu, C.Y., Wu, C.W., Wu, Y.C., Hung, C.S., Yang, A.C., Liu, P.Y., Biswal, B., Lin, C.P., 2014. Local awakening: regional reorganizations of brain oscillations after sleep. Neuroimage 102 (Pt 2), 894–903.
van den Heuvel, M.P., Sporns, O., 2013. Network hubs in the human brain. Trends Cognit. Sci. 17, 683–696.
Vanhaudenhuyse, A., Noirhomme, Q., Tshibanda, L.J., Bruno, M.A., Boveroux, P., Schnakers, C., Soddu, A., Perlbarg, V., Ledoux, D., Brichant, J.F., Moonen, G., Maquet, P., Greicius, M.D., Laureys, S., Boly, M., 2010. Default network connectivity reflects the level of consciousness in non-communicative brain-damaged patients. Brain 133, 161–171.
Wilson, R.S., Mayhew, S.D., Rollings, D.T., Goldstone, A., Przezdzik, I., Arvanitis, T.N., Bagshaw, A.P., 2015. Influence of epoch length on measurement of dynamic functional connectivity in wakefulness and behavioural validation in sleep. Neuroimage 112, 169–179.
Windt, J.M., Nielsen, T., Thompson, E., 2016. Does consciousness disappear in dreamless sleep? Trends Cognit. Sci. 20, 871–882.
Yan, C.G., Craddock, R.C., He, Y., Milham, M.P., 2013. Addressing head motion dependencies for small-world topologies in functional connectomics. Front. Hum. Neurosci. 7, 910.
Yeo, B.T., Krienen, F.M., Sepulcre, J., Sabuncu, M.R., Lashkari, D., Hollinshead, M., Roffman, J.L., Smoller, J.W., Zollei, L., Polimeni, J.R., Fischl, B., Liu, H., Buckner, R.L., 2011. The organization of the human cerebral cortex estimated by intrinsic functional connectivity. J. Neurophysiol. 106, 1125–1165.
Zhang, J., Huang, Z., Chen, Y., Zhang, J., Ghinda, D., Nikolova, Y., Wu, J., Xu, J., Bai, W., Mao, Y., Yang, Z., Duncan, N., Qin, P., Wang, H., Chen, B., Weng, X., Northoff, G., 2018a. Breakdown in the temporal and spatial organization of spontaneous brain activity during general anesthesia. Hum. Brain Mapp. 39, 2035–2046.
Zhang, L., Luo, L., Zhou, Z., Xu, K., Zhang, L., Liu, X., Tan, X., Zhang, J., Ye, X., Gao, J., Luo, B., 2018b. Functional connectivity of anterior insula predicts recovery of patients with disorders of consciousness. Front. Neurol. 9, 1024.
Zilio, F., Gomez-Pilar, J., Cao, S., Zhang, J., Zang, D., Qi, Z., Tan, J., Hiromi, T., Wu, X., Fogel, S., Huang, Z., Hohmann, M.R., Fomina, T., Synofzik, M., Grosse-Wentrup, M., Owen, A.M., Northoff, G., 2021. Are intrinsic neural timescales related to sensory processing? Evidence from abnormal behavioral states. NeuroImage 226, 117579.